

Ashura Particles: Experimental and Theoretical Approaches for Creating Phase-Separated Structures of Ternary Blended Polymers in Three-Dimensionally Confined Spaces

Yutaro Hirai,[†] Edgar Avalos,^{*,‡,§} Takashi Teramoto,^{*,§} Yasumasa Nishiura,^{*,‡} and Hiroshi Yabu^{*,†,§}

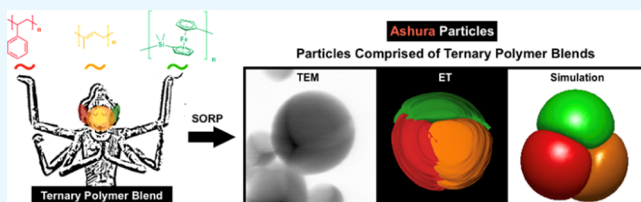
[†]Device/System Group, WPI-Advanced Institute for Materials Research (AIMR), Tohoku University, 2-1-1, Katahira, Aoba-Ku, Sendai 980-8577, Japan

[‡]Mathematical Science Group, WPI-Advanced Institute for Materials Research (AIMR) and MathAM-OIL, Tohoku University and AIST, 2-1-1, Katahira, Aoba-Ku, Sendai 980-8577, Japan

[§]Department of Mathematics, Asahikawa Medical University, 2-1-1-1, Midorigaoka-higashi, Asahikawa 078-8510, Japan

Supporting Information

ABSTRACT: Unique morphologies were found in binary and ternary polymer blended particles, including Ashura-type phase separation, which has three different polymer components on the particle surface. The morphologies of phase-separated structures in the binary polymer blended particles are discussed in terms of the surface tensions of the blended polymers. Structural control of ternary polymer blended particles was achieved based on the combination of polymers by examining binary polymer blended particles. A theoretical approach based on the Cahn–Hilliard equations gives identical morphologies with the experimental results. This work opens the way to creating polymer particles with sophisticated nanostructures by controlling their morphologies as predicted by theoretical simulations.



INTRODUCTION

Nanostructured polymer particles have received considerable attention because of their potential for use in applications for novel photonic materials,¹ pigments for electric papers,² drug carriers for delivery systems,³ probes for immunoassay systems,⁴ and others.^{5,6} For these polymer particles to be suitable for these applications, control over the fine structures of the particles is a central issue. Several techniques have been developed to prepare nanostructured polymer particles. For example, a microfluidic device, which can produce monomers or cross-linkable polymer droplets, is a powerful tool for producing multiphase particles whose sizes are normally over tens of micrometer scale.⁷ Nisisako et al. have reported that Janus-type polymer particles can be formed from a binary mixture of monomer droplets containing different pigments by using a top-down microfluidic device and applied them to electric paper pigments.⁸ Multiple-phase particles can also be prepared from a multiple set of laminar flows in a microfluidic device.⁹ However, using these top-down approaches, it is difficult to fabricate particles of less than micrometer size, required for many of the applications of nanostructured polymer particles mentioned above.

To produce particles of size less than the micrometer scale, emulsion-based bottom-up approaches have been employed to encapsulate polymer blends in small submicron-sized confined spaces. As an example, mini-emulsion formation from binary polymer blends followed by solvent evaporation has been employed to prepare polymer blended particles. Landfester

and co-workers reported the formation of particles composed of donor–accepter-type π -conjugated polymer blended particles.¹⁰ Okubo and co-workers have also presented polymer blended particles from various homopolymers.^{11,12}

We have developed a simple method for fabricating polymer blended particles by a simple mixing of a poor solvent into a solution of polymer blends followed by evaporation of a good solvent.¹³ Using this self-organized precipitation (SORP) process, various kinds of binary polymer blended particles have been prepared. Based on these prepared particles, we have found that binary polymer blended systems can be classified into two kinds of morphologies: Janus and core–shell.¹⁴ Janus-type particles typically have two different surfaces. They consist of two different polymer phases separated in a single particle, forming two respective hemispheres.¹⁵ In the core–shell particle type, one polymer covers the whole surface of the other polymer.¹⁶ Using the SORP method, when the polymers in the blend have similar hydrophobicities, Janus-type phase-separated structures are formed when water was used as the poor solvent. In contrast, the core–shell type phase separation was observed when the hydrophobicity of the polymers was very different. Thus, the structural variety of binary polymer blends is limited to only these two phases, though there are some intermediate structures, such as an engulfment type.

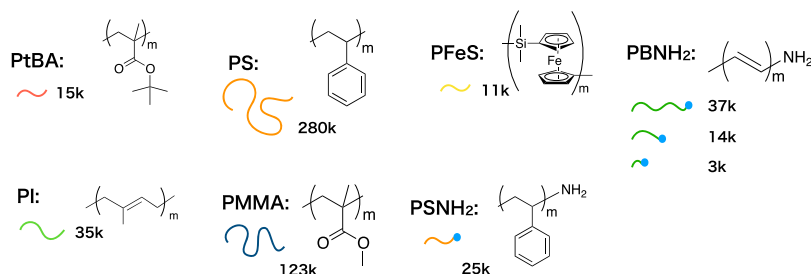
Received: April 7, 2019

Accepted: June 24, 2019

Table 1. Polymers Used in This Experiment

name	abbreviation	M_n [kg/mol]	M_w/M_n	surface tension [mN/m]
poly(1,4-isoprene)	PI	35	2.46	29.4
polystyrene	PS	280	2.12	34.3
poly(<i>tert</i> -butyl methacrylate)	PtBA	15	1.25	36.5
amino-terminated poly(butadiene)	PBNH ₂ -37k	37	1.22	36.6
poly(ferrocenyl dimethylsilane)	PFeS	11	1.17	39.6
amino-terminated poly(butadiene)	PBNH ₂ -14k	14	1.8	41.6
poly(methyl methacrylate)	PMMA	123	1.15	44.7
amino-terminated polystyrene	PSNH ₂	25	1.04	61.8

Scheme 1. Chemical Structures of Polymers



Changing the fraction of the polymer produces changes in the volume fraction of the polymer. However, Janus or core-shell morphologies remain unchanged.¹⁵ Some other examples of Janus,³¹ composite Janus,³² core-shell,³³ and virus-like morphologies³⁴ have been examined.

In order to introduce structural variety for polymer blended particles, increasing the number of polymers in the blend can realize multiphase particles. In this report, we examined studies of binary polymer blended systems prepared by the SORP method to determine the morphologies of the structures produced from the blended polymers. We then investigated structural control of ternary blended particles based on the relationship between the phase-separated structures and the combination of polymers in the binary systems. We found new types of phase-separated polymer blended particles including the “Ashura” type, which has three different polymer components on the surface, named after the Asian god who has three faces. Experimental characterization of such ternary blended polymers has been achieved using state-of-the-art electron tomography (ET), and a numerical simulation based on the coupled Cahn–Hilliard equation was conducted. We discuss the phase behaviors of ternary polymer blended particles in terms of the relationships of the boundary conditions between the polymers and solvents.

RESULTS AND DISCUSSION

Binary and ternary polymer blended particles are prepared by SORP.¹³ The same amounts of tetrahydrofuran (THF) solution of different polymers were mixed and then the same amount of water was mixed into the solution. After evaporation of THF, polymer blended particles precipitated in water. The information and chemical structures of polymers used are listed in Table 1 and Scheme 1, respectively. Typically, submicron- to micron-sized polymer particles were prepared (see Supporting Information S1).

Before preparing the ternary blend particles, the relationship between the phase-separated structures and the combination of polymers was examined based on the binary systems (Figure 1). In order to visualize the internal structures of binary

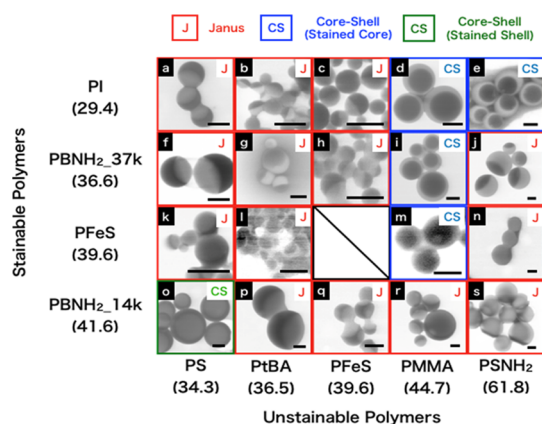


Figure 1. TEM images of obtained binary polymer blended particles. PI, PB-NH₂-37k, and PB-NH₂-14k were stained with OsO₄. PFeS and stained moieties are shown as dark contrasts. The particle morphologies were classified as Janus (red), core-shell (stained core) (blue), and core-shell (stained shell) (green). The surface tensions of the polymers are shown under the names of the polymers. The scale bar indicates 500 nm.

polymer blended particles, stainable polymers with OsO₄ (e.g., PI) or polymers having high electron density [e.g., poly(ferrocenyl dimethylsilane) (PFeS)] were used as the first polymer, and lower electron density polymers were used as the other polymer. In Figure 1, the polymers are ordered based on their surface tensions, which were estimated from measurements of the water and diiodomethane contact angles on the respective polymer films (Supporting Information S2). The structures were classified into three typical types: Janus (red), core-shell (stained core) (blue), and core-shell (stained shell) (green).

The combinations of hydrophobic polymers, which have low surface tensions, typically form the Janus structure (Figure 1a–c,f–h,k,l). Binary polymer blends comprised a combination of low and high surface tension polymers show the core-shell morphology. When the stainable polymer has low surface tension, the unstained polymer forms the shell to stabilize the

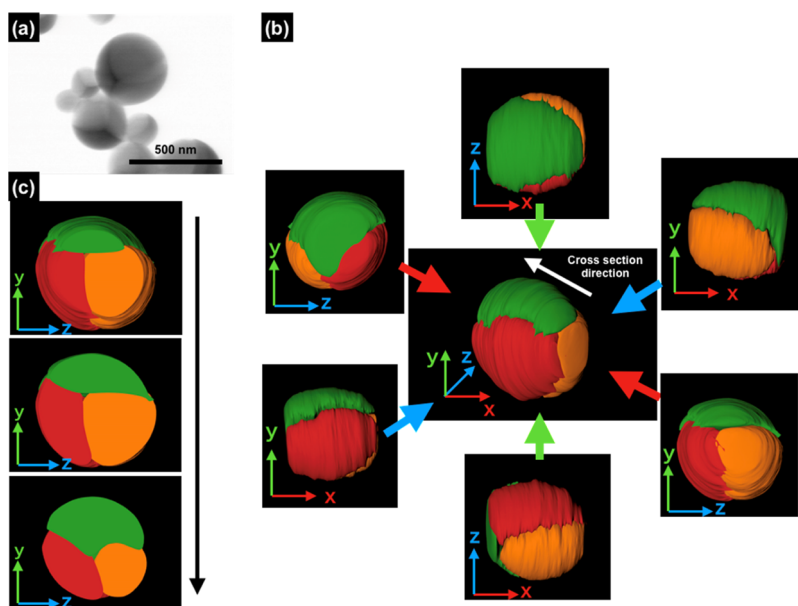


Figure 2. TEM (a), ET (b), and cross-sectional ET (c) images of particles comprised of PS/PI/PFeS, respectively.

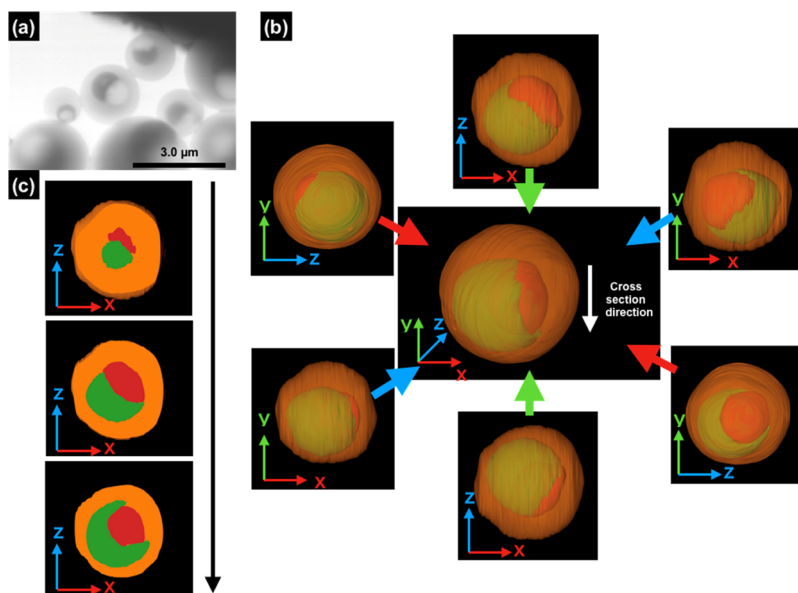


Figure 3. TEM (a), ET (b), and cross-sectional ET (c) images of particles comprising PI/PtBA/PSNH₂, respectively.

interface between the polymer and the dispersion media, water in this case (Figure 1d,e,i,m). In contrast, when the stainable polymer has a high surface tension, stained shells were formed (Figure 1o). These results are identical to those in the previous literature. Moreover, it is noteworthy that the Janus structure was formed from both hydrophilic combinations (Figure 1r,s). There are some exceptions (Figure 1j,n,p,r), however, these results strongly imply that the surface tension of polymers is a key issue for controlling the interior structures of binary polymer blended particles. There are some odd structures found. For example, Figure 1j,n should be core-shell-type phase separation based on the relationships among these polymer combinations, but actually, Janus-type particles were formed. There are some reports about formation of spherical particles that comprised amphiphilic end-functionalized polymer blends.³¹ In those cases, polymers were precipitated in O/W emulsion followed by solvent evaporation, thus,

hydrophilic end groups strongly interact with one another, and the polymers behave more hydrophobic than the original amphiphilic polymers. As seen in the previous reports, both of amphiphilic polymers which have hydrophilic moieties behave as hydrophobic polymers, and the difference of interfacial tensions between two polymers depressed, and as a result, they form Janus-type phase separation.

To investigate possible improvements on morphological controllability, ternary polymer blended systems, consisting of three different polymers, were examined. To study the control of the structure of the ternary system, the interactions among the three different polymers need to be taken into account. First, PS, PI, and PFeS, which have low surface tensions, were used to form ternary blended particles. In the experimental results of the binary polymer blended system shown in Figure 1, PS/PI, PI/PFeS, and PS/PFeS all form Janus-type phase separation structures, indicating that these three polymers have

almost the same interfacial interactions with each other and with water as the dispersion medium. Figure 2a shows a transmission electron microscopy (TEM) image of PS/PI/PFeS ternary blended particles. The image shows that spherical particles were formed and three fan-type domains with different contrasts were clearly imaged inside the particles. Because the contrast of TEM indicates the electron density of the materials, the morphologies and location of the polymers can be distinguished by the difference in the image contrast. The PI moieties that were stained with a heavy metal Os showed the darkest contrast. Because of the high electron density of iron atoms in ferrocene moieties, PFeS also showed a dark contrast, though less than that of the PI phase. PS moieties have low electron density and showed a bright contrast. Therefore, the image indicates that the respective polymers form identical fan-type domains inside the particles. Figure 2b,c shows an ET image and a cross-sectional ET image of the particle, respectively. The PS, PI, and PFeS domains are indicated by red, orange, and green, respectively. Three different domains fill the particle and the particle has surfaces that comprise three different polymer materials. We named these kinds of particles having three different faces “Ashura”, which is the name of an Asian god who has three different faces.

In contrast to the case of the PS/PI/PFeS blend, a core-shell-type phase separated structure should be formed of a combination of low surface tension polymers (e.g., PI, PtBA) and high surface tension polymers [e.g., poly(methyl methacrylate) (PMMA), PSNH₂] based on the results for binary blended systems. Figure 3a shows a TEM image of PI/PtBA/PSNH₂ blend particles. Spherical particles were formed and a core-shell structure was clearly imaged. Surprisingly, for ternary polymer blends, two phases co-exist in the core phase. Because PI/PSNH₂ and PtBA/PSNH₂ particles form a core-shell-type phase separation and PI/PtBA forms a Janus-type phase separation in binary blended particles, it is found that dark contrast PI and bright contrast PtBA form the core and gray PSNH₂ forms the shells. In the core, the PI and PtBA phases form a Janus-type phase separation, as for the binary blended case. Figure 3b,c shows an ET and a cross-sectional ET image of a PI/PtBA/PSNH₂ particle. The PSNH₂ phase completely encapsulates the PI and PtBA phases, which form a binary Janus-type phase separation structure in the core. These results for ternary blended polymer particles indicate that the internal phase separated structures of ternary blended polymers in a three-dimensionally confined space can be controlled based on the surface tension of the polymers. (See also Supporting Information S4).

Simulation of three-dimensional (3D) confinement of nanoparticles is a topic of great interest, as it allows the exploration of a variety of settings.^{19–25} In previous studies of the 3D confinement of diblock copolymer particles, we developed a model of phase separation in a particle based on the coupled Cahn–Hilliard equations.²⁶ This model is a powerful tool for simulating and estimating phase separation morphologies of diblock copolymers in 3D confined systems. There are some differences between the diblock copolymer and polymer blend cases. For example, the interaction between the polymers in polymer blends is weaker than those in diblock copolymers because there are no chemical bonds between these polymers. Furthermore, because we examined ternary blended systems in our experiment, the interactions between the three different phases and the dispersion media had to be

taken into account. Therefore, we developed a new model for ternary blended polymer particles based on the coupled Cahn–Hilliard equations.

Here, we summarize the theoretical model for simulating confined Ashura and Janus core-shell particles. A similar model for the mixture of two systems has been previously described in refs.^{25–27} To describe the particles under study, we need four components, namely, a confinement surface to keep the particle located in a section of the spatial domain and three inner components within the surface. The first component is described by an order parameter u . This order parameter has a value within the interval $[-1, 1]$, where the end points of the interval correspond to solvent-rich domain (-1) and a polymer-rich domain ($+1$). The boundary between the solvent- and polymer-rich domains defines the boundary of the particle. The remaining components are described by order parameters v , w , and z , which define the state of a polymer (nonrich and rich) with values in the interval $[-1, 1]$ with the end points corresponding to the rich and nonrich phases, respectively.

When the four order parameters above interact, a macro-phase separation described by u generates a region in which a confined particle can be located and surrounded by the solvent. Then, three microphase separations take place inside the separated domain. Here, we consider microphase separations of two kinds, namely, Ashura and Janus core-shell.

The main difference between Ashura and Janus core-shell particles is in the way their constitutive components interact with one another. In the Ashura case, all the components interact in the same way, whereas the components of the Janus core exhibit an opposite interaction from the component representing the shell.

The dynamics of the state of the four equations evolves to minimize the value of the energy functional in the following expression^{28–30}

$$F \equiv F_{\epsilon_u \epsilon_v \epsilon_w \epsilon_z}(u, v, w, z) = \int_{\Omega} \left\{ \frac{\epsilon_u^2}{2} |\nabla u|^2 + \frac{\epsilon_v^2}{2} |\nabla v|^2 + \frac{\epsilon_w^2}{2} |\nabla w|^2 + \frac{\epsilon_z^2}{2} |\nabla z|^2 + W(u, v, w, z) \right\} dr \quad (1)$$

where

$$W(u, v, w, z) = \frac{(u^2 - 1)^2}{4} + \frac{(v^2 - 1)^2}{4} + \frac{(w^2 - 1)^2}{4} + \frac{(z^2 - 1)^2}{4} + b_1 u(v + w + z) + b_2 u(v^2 + w^2 + z^2) + b_3 (\pm vw \pm vz - wz) + b_4 (vwz) + b_5 v(w^2 + z^2) \quad (2)$$

The plus and minus signs for the vw and vz terms of eq 2 apply for Janus core-shell and Ashura, respectively. $b_i < 0$ for $i = 1, 2, 3, 4$ and 5 .

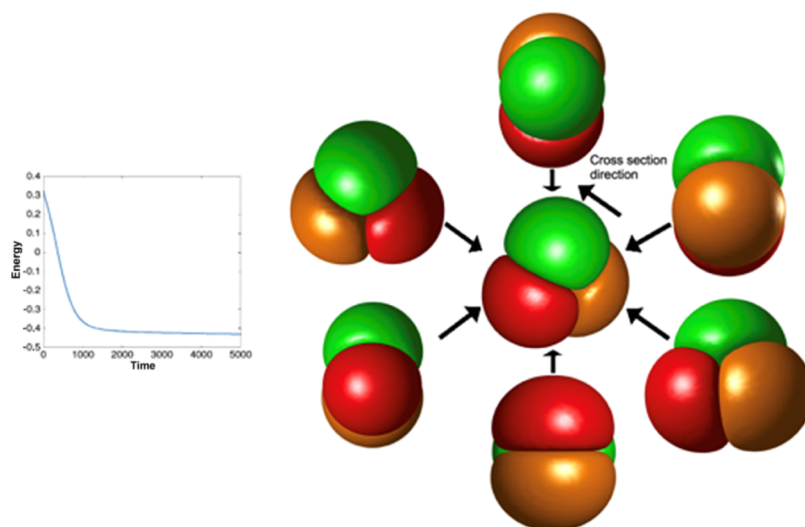


Figure 4. Results of the numerical solution of eqs 7–10 in three dimensions for the Ashura particle. From left to right: energy of steady morphology of the particles in three dimensions and 3D images of Ashura. Parameters: $\epsilon_u = 0.08$, $\epsilon_v = \epsilon_w = \epsilon_z = 0.04$, $b_1 = -0.08$, $b_2 = -0.8$, $b_3 = -0.4$, $b_4 = -0.5$, $b_5 = 0.0$, $\tau_u = \tau_v = \tau_w = \tau_z = 1.0$. The system size is $|\Omega| = 0.8^3$ and the space and time discretized intervals, Δx and Δt , are set to 0.02 and 4×10^{-5} , respectively. All units are dimensionless.

We can write the dynamical equations as

$$\tau_u \dot{u} = -\nabla^2 \left(\epsilon_u^2 \nabla^2 u - \frac{\partial W}{\partial u} \right) \quad (3)$$

$$\tau_v \dot{v} = -\nabla^2 \left(\epsilon_v^2 \nabla^2 v - \frac{\partial W}{\partial v} \right) \quad (4)$$

$$\tau_w \dot{w} = -\nabla^2 \left(\epsilon_w^2 \nabla^2 w - \frac{\partial W}{\partial w} \right) \quad (5)$$

$$\tau_z \dot{z} = -\nabla^2 \left(\epsilon_z^2 \nabla^2 z - \frac{\partial W}{\partial z} \right) \quad (6)$$

After computing the derivatives of eqs 3–6, the gradient system of the equations corresponding to the energy functional is the following set of four coupled Cahn–Hilliard equations as follows

$$\tau_u \dot{u} = \nabla^2 (-\epsilon_u^2 \nabla^2 u + u^3 - u + b_1(v + w + z) + b_2(v^2 + w^2 + z^2)) \quad (7)$$

$$\tau_v \dot{v} = \nabla^2 (-\epsilon_v^2 \nabla^2 v + v^3 - v + b_1 u + 2b_2 uv + b_3(\pm w \pm z) + b_4 wz + b_5(w^2 + z^2)) \quad (8)$$

$$\tau_w \dot{w} = \nabla^2 (-\epsilon_w^2 \nabla^2 w + w^3 - w + b_1 u + 2b_2 uw + b_3(\pm v - z) + b_4 vz + 2b_5 vw) \quad (9)$$

$$\tau_z \dot{z} = \nabla^2 (-\epsilon_z^2 \nabla^2 z + z^3 - z + b_1 u + 2b_2 uz + b_3(\pm v - w) + b_4 vw + 2b_5 vz) \quad (10)$$

In eq 1, Ω is a smooth bounded domain in \mathbb{R}^N . Here, we focus on three-dimensional confinement and thus $N = 3$. Parameters ϵ_u , ϵ_v , ϵ_w , and ϵ_z are proportional to the thickness of the propagating fronts of each component. These parameters control the size of the interface of the order parameters u , v , w , and z , respectively. The multidimensional double-well potential in eq 2 represents two different possible states in

phase transition, -1 or $+1$. This function has four dimensions and the coupling parameters b_1 , b_2 , b_3 , b_4 and b_5 .

Coupling parameter b_1 controls the affinity of the surrounding medium represented by order parameter u and each of the components of the particle in such a way that as the magnitude of b_1 increases, the preference of u for the components v , w , and z also increases accordingly. For simplicity, we assume that the constitutive components of the particle (Ashura or Janus core–shell) interact with the solvent with equal intensity. Parameter b_2 is a confinement parameter. The term in eq 2 associated to b_2 lowers the energy when $u > 0$ (polymer rich). Intuitively, this parameter helps to confine the particle to a polymer-rich region and to keep it separated from the solvent. Parameter b_3 can be related to the surface tension between the components of the particle. In the case of Ashura, all the three pairs of components, (v, w) , (w, z) , and (v, z) , have a similar value of surface tension, thus, they form flat interfaces of approximately equal size. The case for Janus core–shell particles is different. In Janus core–shell particles, the shell and the core have considerably large interfacial tension, which explains the spherical interface between the shell and core. In contrast, the components in the Janus core have a small interfacial tension between them, and therefore, these components form a small flat interface. To account for the difference of interfacial tensions between components in Ashura particles and between shell and core components in the Janus core–shell particles, we employ opposite signs in terms of eq 2 associated to b_3 . Parameter b_4 is related to the triple junction between components v , w , and z . Parameter b_5 is a secondary confinement parameter that is zero for the Ashura particle. In the case of the Janus core–shell particle, the term in eq 2 associated to b_5 lowers the energy when $v > 0$. Intuitively, this parameter helps to confine the Janus core to a region localized under a shell defined by $v > 0$. Notice that while parameter $b_2 < 0$ promotes microphase separation when $u > 0$, parameter $b_3 < 0$ promotes microphase separations when $v > 0$. Parameters τ_u , τ_v , τ_w , and τ_z are time constants to control the speed at which order parameter u , v , w , and z move.

Equations 7–10 constitute a mixture of the four coexisting order parameters u , v , w , and z . The first equation, featuring

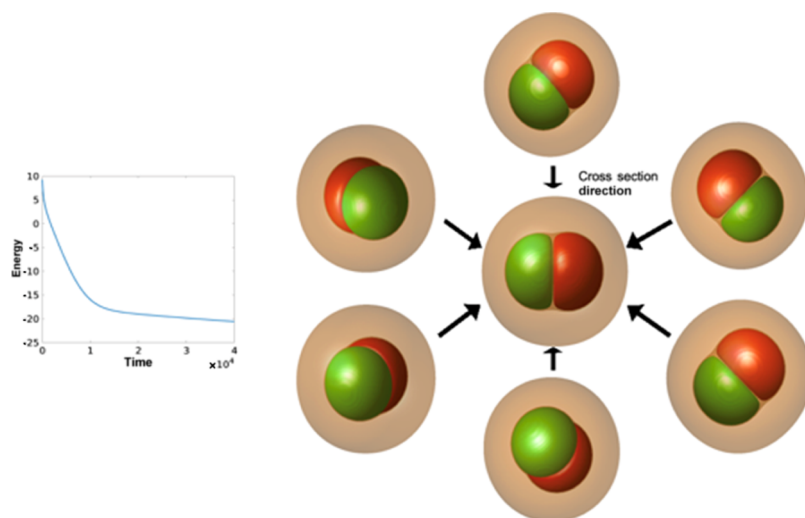


Figure 5. Results of the numerical solution of eqs 7–10 in three dimensions for the Janus core–shell particle. From left to right: energy of steady morphology of the particles in three dimensions and 3D images of Janus core–shell. Parameters: $\epsilon_u = \epsilon_v = \epsilon_w = \epsilon_z = 0.04$, $b_1 = -0.10$, $b_2 = -0.8$, $b_3 = -0.05$, $b_4 = -0.2$, $b_5 = -0.05$. The other settings are $|\Omega| = 2.0^3$, $\Delta x = 0.02$, and $\Delta t = 2 \times 10^{-5}$. All units are dimensionless.

the shape variable, separates a confined particle from the surrounding external medium. The other three equations represent the inner components of the nanoparticle. This proposed approach allows us to describe a particle by integrating a set of equations for the whole system, thus avoiding the explicit treatment of the boundary conditions at each interface.

Figures 4 and 5 show numerical results for Ashura and Janus core–shell particles in three dimensions. The Ashura particle seems to be energetically stable. With regard to Janus core–shell particles, although these morphologies are observable in experiments, our simulation results suggest that they appear to be transient in the framework of our theoretical model. Specifically, Janus core–shell particles in three dimensions undergo barely noticeable changes in energy over a long time period. However, in two dimensions, these particles sustain a configuration that is comparable in shape to the experimental findings during a time period and the stability of this morphology can be maintained to some extent by thermal annealing.

Supporting Information S3 shows differences of interfacial tensions between pairs of polymers. The interfacial tension is a measure of the energy content at the interface of the polymers. In the case of the Ashura particle, the constitutive components have low values of interfacial tension, 0.26, 0.714, and 1.15 (Table S3); therefore, it is expected to have small interfaces in this case. This explains the flat interfaces of the polymers in the Ashura particle. For the Janus core–shell particle, the components at the core (Janus) have a small value of interfacial tension (0.377), which again is related to the flat interface of the components at the core of the particle. However, the shell and the core have quite a large interfacial tension (23.1 and 26.3). This large energy content at the interface explains the large size of such interface between the shell and the core, which completely engulfs the core. As for the model, the b_3 term in the potential for the Ashura particle is $-vw - vz - wz$. Each factor in this term has the same low intensity of the interfacial tension (this just for simplicity). On the other hand, the b_3 term for the case of the Janus core shell is $vw + vz - wz$. The intensity of this term at the core ($-wz$) is

much smaller than the interactions between the core and the shell (vw and vz).

CONCLUSIONS

The experimental and simulation results are identical, showing that the model correctly simulates the experimental results. Actually, we have experimentally examined rational 21 combinations (19 for binary and 2 for ternary) of polymers to reveal the effect of interfacial tensions on phase-separated structures in the polymer blended particles, and these data have been summarized in three figures. To ensure the reproducibility of the structures found, we performed and analyzed a large number of experiments and more than 200 TEM images were studied. In this work, we report the Ashura-type particle in the ternary blended system, which to the best of our knowledge, has not been previously shown. These results also suggest that ternary blended polymer particles exhibit new types of morphologies and the combination of the polymers gives rise to a variety of morphologies. The ternary blended system provides a simple way to fabricate particles possessing sophisticated morphologies that can be applied to a wide variety of practical applications.

EXPERIMENTAL METHODS

Materials. Polystyrene (PS, $M_w = 280k$) and cis-type polyisoprene (PI, $M_w = 35k$) were purchased from Aldrich. Poly(*tert*-butylacrylate) (PtBA, $M_n = 15k$), PFeS ($M_n = 11k$), PMMA ($M_n = 123k$), poly(1,2-butadiene) amino-terminated polystyrene (PBNH₂, $M_n = 14k$, 37k), and amine-terminated polystyrene (PSNH₂, $M_n = 25k$) were purchased from Polymer Source Inc. THF was purchased from FUJIFILM Wako Pure Chemical.

Preparation of Binary Polymer Blended Particles. The polymer blended particles were prepared according to the literature. Each polymer was dissolved in THF to prepare a 0.1 mg/mL solution. Two polymer solutions (0.5 mL) were mixed, and then, 1 mL water was added to the solution with a speed of 1 mL/min. THF was evaporated from the mixed solution in a glass bottle immersed in a water bath at 40 °C for 12 h. The solution became gradually turbid with evaporation of

THF and finally, aqueous dispersions of binary polymer blended particles were obtained. PI- or PBNH₂- containing particles were treated with 0.2% OsO₄ aq. for 2 h to stain the polymer and to form cross-linked double bonds of PI and PB moieties. After staining, the particles were corrected by ultracentrifugation (12 000 rpm, 15 min) and washed with pure water three times.

Preparation of Ternary Polymer Blended Particles.

The ternary polymer blended particles were prepared in the same way as the binary polymer blends. Three different polymer solutions (0.33 mL) were mixed and then 1 mL of water was added to the solution. Other procedures were also the same as for binary polymer blends.

STEM Observations. Cu grids with an elastic carbon membrane were hydrophilized with UV–O₃ treatment for 5 min. One drop of an aqueous dispersion of particles was dropped onto a grid surface and dried at room temperature. The structure of the particles was observed using a scanning electron microscope (S-5200, Hitachi, Japan) equipped with a scanning TEM (STEM) unit.

ET Observations. Cu grids were prepared as for STEM observations. The samples were observed by using a transmission electron microscope (H-7650, Hitachi, Japan) with varying tilt angles from –60° to 60° with a step of 1° (120 images were obtained). The obtained images were stacked using the imaging software ImageJ (ver. 1.48v, NIH, United States), and then, tilting axis alignment and reconstruction of *xy* sliced images were performed using a plug-in for ImageJ, TomoJ (freely provided by Centre Universitaire d'Orsay, France).¹⁷ The generation of 3D reconstruction images and abstraction of outlines were performed using HawkC, which was freely provided by Osaka University, Japan.¹⁸ Cross-sectional images and reconstruction of the 3D images were generated using CINEMA 4D (MAXON Computer, GmbH, Germany).

Theoretical Simulation and Numerical Details. To integrate eqs 7–10, we implemented a semi-implicit scheme using appropriate parameters in Figures 4 and 5. We initiated the simulation from suitable initial conditions for each component. The numerical solution of the coupled system of equations guarantees the production of morphologies of minimum free energy for a sufficiently long simulation time. Likewise, the solution of the Cahn–Hilliard equations ensures that the total volume

$$(1/|\Omega|) = \int_{\Omega} u_0 \, dV \quad (11)$$

remains constant, where u_0 is the initial distribution of the component u in the whole domain. We selected appropriate values for the parameters of the model and solved the dynamical equations in three dimensions. For a simulation cell in three dimensions, we use a cubic lattice with periodic boundary conditions in the X -, Y -, and Z -axes of the lattice box. To represent three-dimensional morphologies, we plotted isosurfaces taken at appropriate values of v , w , and z .

■ ASSOCIATED CONTENT

● Supporting Information

The Supporting Information is available free of charge on the ACS Publications website at DOI: 10.1021/acsomega.9b00991.

Polymer blended particles, measurement of surface tensions of polymers, ET, and simulated models of Ashura and core–shell Janus-type particles (PDF)

■ AUTHOR INFORMATION

Corresponding Authors

*E-mail: soyedgaravalos@gmail.com (E.A.).
 *E-mail: teramoto@asahikawa-med.ac.jp (T.T.).
 *E-mail: yasumasa@pp.ij4u.or.jp (Y.N.).
 *E-mail: hiroshi.yabu.d5@tohoku.ac.jp (H.Y.).

ORCID

Edgar Avalos: 0000-0002-3009-6176

Hiroshi Yabu: 0000-0002-1943-6790

Funding

This work was partially supported by KAKENHI Grants-in-Aid (nos. 17H01223, 18H05322 and 18H05482) and JSPS A3 Foresight Program from the Japan Society for the Promotion of Science (JSPS), Ministry of Education, Culture, Sports, Science and Technology (MEXT), Japan, and by AMED-SENTAN (no. 16809277). This work was also supported by the Fusion Research and Advanced Target Project of WPI-AIMR, Tohoku University. E.A. and Y.N. gratefully acknowledge the support of the Council for Science, Technology and Innovation (CSTI), Cross-ministerial Strategic Innovation Promotion Program (SIP), “Structural Materials for Innovation”.

Notes

The authors declare no competing financial interest.

■ ACKNOWLEDGMENTS

Y.H. and H.Y. would like to thank Minori Suzuki and Sachie Kosaka of WPI-AIMR, Tohoku University, for assistance with STEM observations.

■ REFERENCES

- (1) Akcora, P.; Liu, H.; Kumar, S. K.; Moll, J.; Li, Y.; Benicewicz, B. C.; Schadler, L. S.; Acehan, D.; Panagiotopoulos, A. Z.; Pryamitsyn, V.; Ganesan, V.; Ilavsky, J.; Thiyagarajan, P.; Colby, R. H.; Douglas, J. F. Anisotropic Self-Assembly of Spherical Polymer-Grafted Nanoparticles. *Nat. Mater.* **2009**, *8*, 354–359.
- (2) Wang, H.; Yang, S.; Yin, S.-N.; Chen, L.; Chen, S. Janus Suprabead Displays Derived From the Modified Photonic Crystals Toward Temperature Magnetism and Optics Multiple Responses. *ACS Appl. Mater. Interfaces* **2015**, *7*, 8827–8833.
- (3) Venkataraman, S.; Hedrick, J. L.; Ong, Z. Y.; Yang, C.; Ee, P. L. R.; Hammond, P. T.; Yang, Y. Y. The Effects of Polymeric Nanostructure Shape on Drug Delivery. *Adv. Drug Delivery Rev.* **2011**, *63*, 1228–1246.
- (4) Lee, S.-W.; Lee, K.-S.; Ahn, J.; Lee, J.-J.; Kim, M.-G.; Shin, Y.-B. Highly Sensitive Biosensing Using Arrays of Plasmonic Au Nanodisks Realized by Nanoimprint Lithography. *ACS Nano* **2011**, *5*, 897–904.
- (5) Kumar, A.; Park, B. J.; Tu, F.; Lee, D. Amphiphilic Janus Particles at Fluid Interfaces. *Soft Matter* **2013**, *9*, 6604.
- (6) Gröschel, A. H.; Walther, A.; Löbbling, T. I.; Schacher, F. H.; Schmalz, H.; Müller, A. H. E. Guided Hierarchical Co-Assembly of Soft Patchy Nanoparticles. *Nature* **2016**, *503*, 247–251.
- (7) Kim, S.-H.; Shim, J. W.; Lim, J.-M.; Lee, S. Y.; Yang, S.-M. Microfluidic Fabrication of Microparticles with Structural Complexity Using Photocurable Emulsion Droplets. *New J. Phys.* **2009**, *11*, 075014.
- (8) Nisisako, T.; Torii, T.; Takahashi, T.; Takizawa, Y. Synthesis of Monodisperse Bicolored Janus Particles with Electrical Anisotropy Using a Microfluidic Co-Flow System. *Adv. Mater.* **2006**, *18*, 1152.

- (9) Dendukuri, D.; Pregibon, D. C.; Collins, J.; Hatton, T. A.; Doyle, P. S. Continuous-Flow Lithography for High-Throughput Micro-particle Synthesis. *Nat. Mater.* **2006**, *5*, 365–369.
- (10) Kietzke, T.; Neher, D.; Landfester, K.; Montenegro, R.; Güntner, R.; Scherf, U. Novel Approaches to Polymer Blends Based on Polymer Nanoparticles. *Nat. Mater.* **2003**, *2*, 408–412.
- (11) Tanaka, T.; Nakatsuru, R.; Kagari, Y.; Saito, N.; Okubo, M. Effect of Molecular Weight on the Morphology of Polystyrene/Poly(Methyl Methacrylate) Composite Particles Prepared by the Solvent Evaporation Method. *Langmuir* **2008**, *24*, 12267–12271.
- (12) Ahmad, H.; Saito, N.; Kagawa, Y.; Okubo, M. Preparation of Micrometer-Sized, Monodisperse “Janus” Composite Polymer Particles Having Temperature-Sensitive Polymer Brushes at Half of the Surface by Seeded Atom Transfer Radical Polymerization. *Langmuir* **2008**, *24*, 688–691.
- (13) Yabu, H.; Higuchi, T.; Ijio, K.; Shimomura, M. Spontaneous Formation of Polymer Nanoparticles by Good-Solvent Evaporation as a Nonequilibrium Process. *Chaos* **2005**, *15*, 047505.
- (14) Yabu, H. Creation of Functional and Structured Polymer Particles by Self-Organized Precipitation (SORP). *Bull. Chem. Soc. Jpn.* **2012**, *85*, 265–274.
- (15) Higuchi, T.; Tajima, A.; Yabu, H.; Shimomura, M. Spontaneous Formation of Polymer Nanoparticles with Inner Micro-Phase Separation Structures. *Soft Matter* **2008**, *4*, 1302.
- (16) Motoyoshi, K.; Tajima, A.; Higuchi, T.; Yabu, H.; Shimomura, M. Static and Dynamic Control of Phase Separation Structures in Nanoparticles of Polymer Blends. *Soft Matter* **2010**, *6*, 1253–1257.
- (17) Messaoudi, C.; Boudier, T.; Sorzano, C.; Marco, S. Tomography Software for Three-Dimensional Reconstruction in Transmission Electron Microscopy. *BMC Bioinf.* **2007**, *8*, 288.
- (18) Nishi, R.; Cao, M.; Kanaji, A.; Nishida, T.; Yoshida, K.; Isakozawa, S. Fast Auto-Acquisition Tomography Tilt Series by Using HD Video Camera in Ultra-High Voltage Electron Microscope. *Microscopy* **2014**, *63*, i25.1.
- (19) Chen, P.; Liang, H.; Shi, A.-C. Origin of Microstructures From Confined Asymmetric Diblock Copolymers. *Macromolecules* **2007**, *40*, 7329–7335.
- (20) Pinna, M.; Guo, X.; Zvelindovsky, A. V. Block Copolymer Nanoshells. *Polymer* **2008**, *49*, 2797–2800.
- (21) Pinna, M.; Guo, X.; Zvelindovsky, A. V. Diblock Copolymers in a Cylindrical Pore. *J. Chem. Phys.* **2009**, *131*, 214902.
- (22) Chen, P.; Liang, H.; Shi, A.-C. Microstructures of a Cylinder-Forming Diblock Copolymer Under Spherical Confinement. *Macromolecules* **2008**, *41*, 8938–8943.
- (23) Pinna, M.; Hiltl, S.; Guo, X.; Böker, A.; Zvelindovsky, A. V. Block Copolymer Nanocontainers. *ACS Nano* **2010**, *4*, 2845–2855.
- (24) Shi, A.-C.; Li, B. Self-Assembly of Diblock Copolymers Under Confinement. *Soft Matter* **2013**, *9*, 1398–1413.
- (25) Higuchi, T.; Pinna, M.; Zvelindovsky, A. V.; Jinnai, H.; Yabu, H. Multipod Structures of Lamellae-Forming Diblock Copolymers in Three-Dimensional Confinement Spaces: Experimental Observation and Computer Simulation. *J. Polym. Sci., Part B: Polym. Phys.* **2016**, *54*, 1702–1709.
- (26) Avalos, E.; Higuchi, T.; Teramoto, T.; Yabu, H.; Nishiura, Y. Frustrated Phases Under Three-Dimensional Confinement Simulated by a Set of Coupled Cahn-Hilliard Equations. *Soft Matter* **2016**, *12*, 5905–5914.
- (27) Avalos, E.; Teramoto, T.; Komiyama, H.; Yabu, H.; Nishiura, Y. Transformation of Block Copolymer Nanoparticles From Ellipsoids with Striped Lamellae Into Onionlike Spheres and Dynamical Control via Coupled Cahn-Hilliard Equations. *ACS Omega* **2018**, *3*, 1304–1314.
- (28) Ohta, T.; Ito, A. Dynamics of Phase Separation in Copolymer-Homopolymer Mixtures. *Phys. Rev. E: Stat. Phys., Plasmas, Fluids, Relat. Interdiscip. Top.* **1995**, *52*, S250–S260.
- (29) Teramoto, T. Three-Dimensional Morphology in Copolymer-Homopolymer Mixtures. *J. Phys. Soc. Jpn.* **2001**, *70*, 3217–3220.
- (30) Teramoto, T.; Nishiura, Y. Morphological Characterization of the Diblock Copolymer Problem with Topological Computation. *Jpn. J. Ind. Appl. Math.* **2010**, *27*, 175–190.
- (31) Tanaka, T.; Okayama, M.; Kitayama, Y.; Kagawa, Y.; Okubo, M. Preparation of “mushroom-like” janus particles by site-selective surface-initiated atom transfer radical polymerization in aqueous dispersed systems. *Langmuir* **2010**, *26*, 7843–7847.
- (32) Arita, T.; Kanahara, M.; Motoyoshi, K.; Koike, K.; Higuchi, T.; Yabu, H. Localization of Polymer-grafted Maghemite Nanoparticles in a Hemisphere of Janus Polymer Particle Prepared by Self-organized Precipitation (SORP) Method. *J. Mater. Chem. C* **2013**, *1*, 207–212.
- (33) Yabu, H.; Koike, K.; Motoyoshi, K.; Higuchi, T.; Shimomura, M. A Novel Route for Fabricating Metal-Polymer Composite Particles with Phase Separation Structures. *Macromol. Rapid Commun.* **2010**, *31*, 1267–1271.
- (34) Hirai, Y.; Wakiya, T.; Yabu, H. Virus-Like Particles Composed of Sphere-Forming Polystyrene-*block*-Poly(*t*-butyl acrylate) (PS-*b*-PtBA) and Control of Surface Morphology by Homopolymer Blending. *Polym. Chem.* **2017**, *8*, 1754–1759.